A Design of Capacitance Sensor System for Void Fraction Measurement in Liquid-Gas flow

Jin-Ming Zhang, Yi-Ping Liu
Shanghai Institute of Measurement and Testing Technology, Shanghai, P.R. China
Tel: 86-021-38839800-36301, Fax: 86-021-50798562, E-mail: yiping3@yahoo.cn

Abstract: The sensors, consisting of METC axial synchro driving guard electrodes and two sets of detecting electrodes, make it possible to obtain simultaneously two groups of signals of the void fraction in liquid-gas two-phase flow. The quality of the reconstructed image and the performance of multielectrode capacitive system depend on the uniformity of sensibility distribution between electrode pairs. To determine the spatial sensitivity distribution over the pipe cross section and to study the static responses of the system, a numerical simulation has been employed to analyze the design parameters and the system performance of the capacitive systems. As a consequence, a prototype of 12-electrode internal sensors with METC configuration is presented as first part of ECT system used in liquid-gas flow void fraction measurement.

Keywords: Liquid-gas flow, Void fraction, Capacitance sensor system

1. Introduction

The liquid-gas multiphase transportation technology, including multiphase pressurization, the multiphase flowmeter and the multiphase flow control, has become much effective as an economic and reliable method for the oil-gas exploitation in the seabed. The prediction of pressure drop, heat transfer coefficients and void fraction is necessary to the design of mixing transportation system and prerequisite to conduct the flow pattern identification. Among those flow parameters, void fraction, defined as the cross section fraction occupied by gas, i.e. $\alpha = A_G / A$, is the most effective one which reflect the flow pattern characteristics[1]. Although much effort has been made on the theoretical computation and empirical formula derived from auxiliary experiment, it is unsuitable to apply them to liquid-gas two-phase flow system in many cases where actual measurement is dominant.

Quick Close Value (QCV) might be the commonest method to measure void fraction directly[2]. Trapped within a section of a pipe by two synchro driving electromagnetic valves, liquid and gas are measured statically to obtain the average void fraction. However, failure to realize real-time measurement prevents its application in industrial production. X-ray absorption, although accurate, is limited in rare applications since its well known radioactive effect. In recent years, there has been growing interest in flow imaging and research works based on neutron[3], gamma-ray[4] and ultra sound[5] techniques have been reported. Electrical capacitive tomography (ECT), as one kind of process tomography technique, has been used comprehensively in medical imaging providing useful means for obtaining instantaneous information on components distribution over a cross section of the pipe. Beck et al.[6] first proposed this technique which has been found to have considerable potential in process control system.

ECT system consists of three core parts (see Fig. 1): capacitance sensors, data acquisition and control system and imaging reconstruction computer. The sensors transform two-phase flow distribution into the capacitive values whose amplitude depends on the dielectric distribution over the cross section of pipeline. The data acquisition and control system receives them in all possible

electrode pairs. Through A/D transformation, the values, as digital signal, are fed into the computer and a cross sectional image of the components distribution is reconstructed by using a linear backprojection (LBP) algorithm.

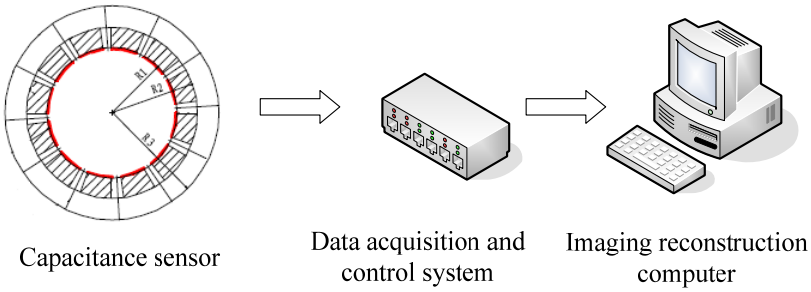

Fig. 1 The basic flow imaging system

In this paper, a capacitance sensor system is presented to measure void fraction in liquid-gas co-current flow. Yang W. Q[7] summarized the features of internal and external electrodes systems (Fig. 2). There are two major structures about axial guard electrodes, one is multielectrode capacitive system with axial synchro driving guard electrodes developed by U.S. Department of Energy, Morgantown Energy Technology Center (METC for short), the other is multielectrode capacitive system with axial earthed guard electrodes developed by the University of Manchester Institute of Science and Technology, abbreviated to UMIST. METC system uses 16 evenly spaced, circumferentially located electrodes at each of four levels evenly spaced along the axis of a 6-inch diameter fluidized bed as the density-sensing elements. During the measurement, the erasable programmable read-only memory (EPROM) section of scan control system is programmed to produce electrode voltage excitation patterns that allow the electrically guarded measurement of the current between all possible pairs of oppositely excited electrodes simultaneously at each level. UMIST system comprises a source electrode (connected to the driving voltage source), a detecting electrode (connected to the virtual earth input of the capacitance measuring circuit) and an earthed screen (which functions to shield the electrode plates from the interference by external electrical fields). In addition, multielectrode capacitive system without axial guard electrodes (non-guard) is studied as a candidate. The system design parameters, such as pipe wall permittivity (ε_{pw}), the permittivity of the conveyed phase (ε), pipe wall thickness (R_2-R_1) and the length of axial guard electrode plate are discussed here to present the sensitivities distribution's influence on the measurement.

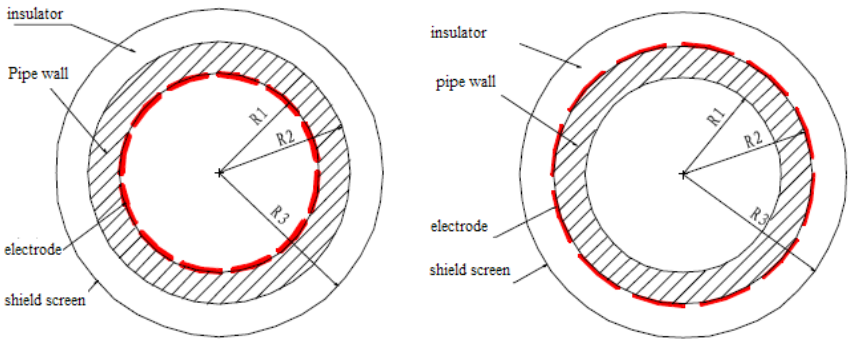

Fig. 2 Internal (left) and external (right) electrodes systems

The quality of the reconstructed image and the performance of multielectrode capacitive system depend on the uniformity of sensibility distribution between electrode pairs[8]. To determine the spatial sensitivity distribution over the pipe cross section and to study the static responses of the

system due to different flow regimes, a numerical simulation is employed to optimize the design parameters and aforementioned system performance of the capacitive systems. FEM has been chosen in current research because its mesh can be designed to fit complex geometries and the system capacitance is easy to compute from the known electrical potential distributions on the system boundary.

2. Finite Element Modelling of Capacitance Sensor System

In prior work, two-dimensional FE modelling of capacitance sensor system was always adopted under the following assumption: The fringing field effects due to the finite length of electrodes are negligible, this assumption implies that the electrode plates and screen are so long that the electric field distribution remains the same for any plane perpendicular to the axial direction of the pipe. However, it is not entirely suitable for most capacitance sensor systems, such as METC and UMIST. In order to get accurate prediction, a three-dimensional FE modelling has been adopted. Basic model and FE mesh layout are shown in Fig. 3. The fringing field effects are taken into account, and the other common assumptions are listed below:

(1) Flow component distribution of a two-phase flow does not change spatially along the pipe axial direction at least not within the electrode length.

(2) Permittivities of flow components remain constant.

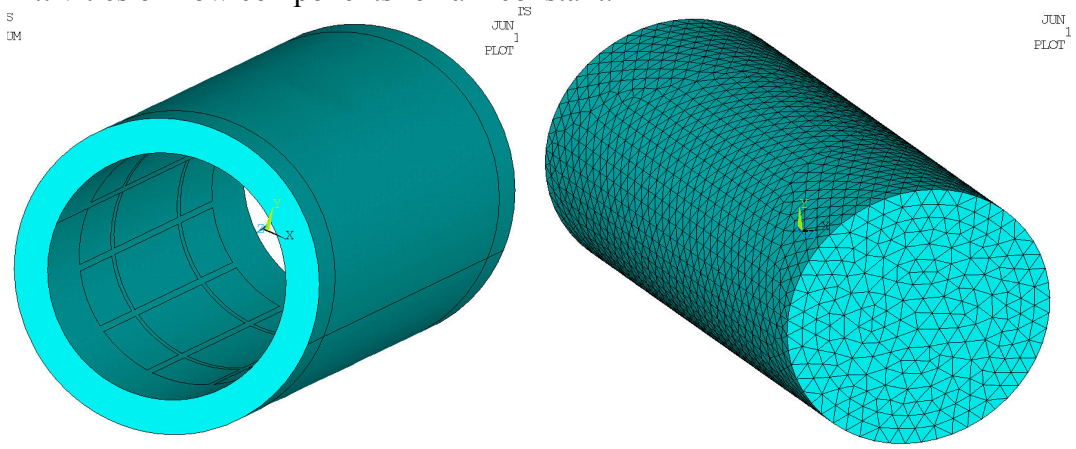

Fig. 3 Finite element model of 12-electrode capacitive system with mesh layout

Under these two assumptions, the potential distribution over cross section can be calculated by Poisson equation with the given dielectric constant distribution. The Dirichlet boundary conditions are also given below:

$$\begin{cases} \nabla \cdot [\varepsilon(x,y,z)\nabla\phi(x,y,z)] = 0 & \\ \phi(x,y,z)\,|_{(x,y,z)\in\Gamma_i} = U & (i = 1,2,\cdots,11) \\ \phi(x,y,z)\,|_{(x,y,z)\in\Gamma_j} = 0 & (j = 2,3,\cdots,12) \\ \phi(x,y,z)\,|_{(x,y,z)\in\Gamma_s} = 0 & \end{cases} \tag{1}$$

where, Γ_s represent the computational domains belonging to the screen, and Γ_i and Γ_j are the spatial locations of *i*th electrode and *j*th electrode respectively, U is the potential difference between given electrodes. According to Thomson's theorem, for specified charges on each of the boundary segments, the stored electrostatic energy is minimum when each of the boundaries is a conductor, i.e., electrically charged particles arrange themselves so as to have the least energy. In result, a numerical functional form of Eq. (1) is given as

$$\begin{cases} J_\phi = \dfrac{1}{2}\iiint\limits_D \varepsilon(x,y,z)E^2 \mathrm{d}V \\ \quad = \iiint\limits_D \dfrac{\varepsilon(x,y,z)}{2}[(\dfrac{\partial\phi(x,y,z)}{\partial x})^2 + (\dfrac{\partial\phi(x,y,z)}{\partial Y})^2 + (\dfrac{\partial\phi(x,y,z)}{\partial Z})^2]\ \mathrm{d}x\ \mathrm{dy}\ \mathrm{dz} = \min \\ \phi(x,y,z)\mid_{(x,y,z)\in\Gamma_i} = U \qquad (i = 1,2,\cdots,11) \\ \phi(x,y,z)\mid_{(x,y,z)\in\Gamma_j} = 0 \qquad (j = 2,3,\cdots,12) \\ \phi(x,y,z)\mid_{(x,y,z)\in\Gamma_s} = 0 \end{cases} \tag{2}$$

where D is the space inside shield screen. Since current task is to facilitate the selection of capacitance sensor system and optimizing system design parameters, it goes along a forward solving process. After the potential distribution is obtained, Gauss law with a numerical integral form, i.e. Eq. (3), is applied to calculate the sense charge on the jth electrode.

$$q_{ij} = \oiiint\limits_{V_j} \varepsilon(x,y,z)\vec{E}(x,y,z)\ \mathrm{d}\vec{V} = -\oiiint\limits_{V_j} \varepsilon(x,y,z)\nabla\phi(x,y,z)\ \mathrm{d}\vec{V} \tag{3}$$

where V_j is the volume enveloping the electrode j. Then the capacitance of electrode pairs i-j can be calculated from Eq. (4):

$$C_{ij} = \frac{q_{ij}}{U} \qquad (i = 1,2,\cdots,11;\ j = 2,3,\cdots,12) \tag{4}$$

3. Results and Discussion

3.1. The Spatial Distribution for Three Capacitive Systems

Fig. 4 shows the potential distributions in the center axial section of three type of sensor. The part between two solid lines represents the detecting electrodes domain. Potential distribution discrepancy is shown by equipotential contours, which appears uniform in METC system, while contours of UMIST and non-guard system seem to be uneven. This computational result means that electrical fields in UMIST and non-screen system tend to disperse along axial direction since the lines of the electric field are perpendicular to the equipotential contours. In contrast, the dispersancy in METC system seems imperceptible. Therefore, as the permittivities of flow components keep constant, it follows that the value attributed to a measurand by METC system should be more accordant with the simulation result than that by UMIST and non-guard system, and such conclusion leads to the selection leaning towards the METC system.

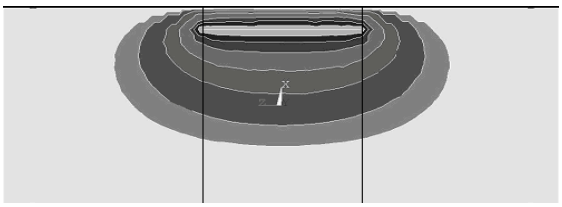

(a) Non-guard electrode

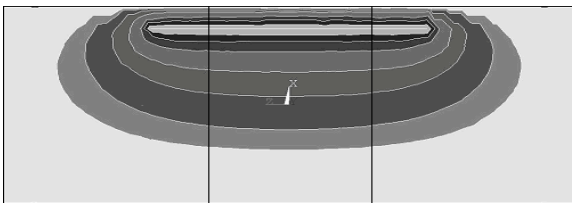

(b) UMIST (L=50 mm)

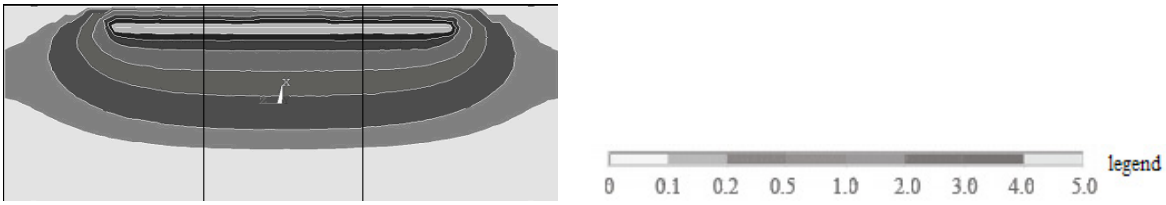

(c) METC(L=50 mm)

Fig. 4 Potential distribution in the center axial section for three types of sensors
L is the length of electrode plate

3.2. Effect of the Length of Guard Electrode on Spatial Potential Distribution

The potential distribution in the center axial section for five different lengths of guard electrode plate, i.e. 20 mm, 30 mm, 50 mm, 70 mm and 100 mm, are shown in Fig. 5. The two solid lines follow the same meaning as mentioned before. Although the potential distribution between the excited and detecting electrodes tends to be even with the increasing length of guard electrode plate, no evident change of the potential distribution between the two detecting electrode plates has been found after the plate length exceeds a certain value. However, longer plate, more expensive overall capacitive system becomes. So, for the pipeline with 125 mm interior diameter, 50 mm long guard electrode is enough for shield.

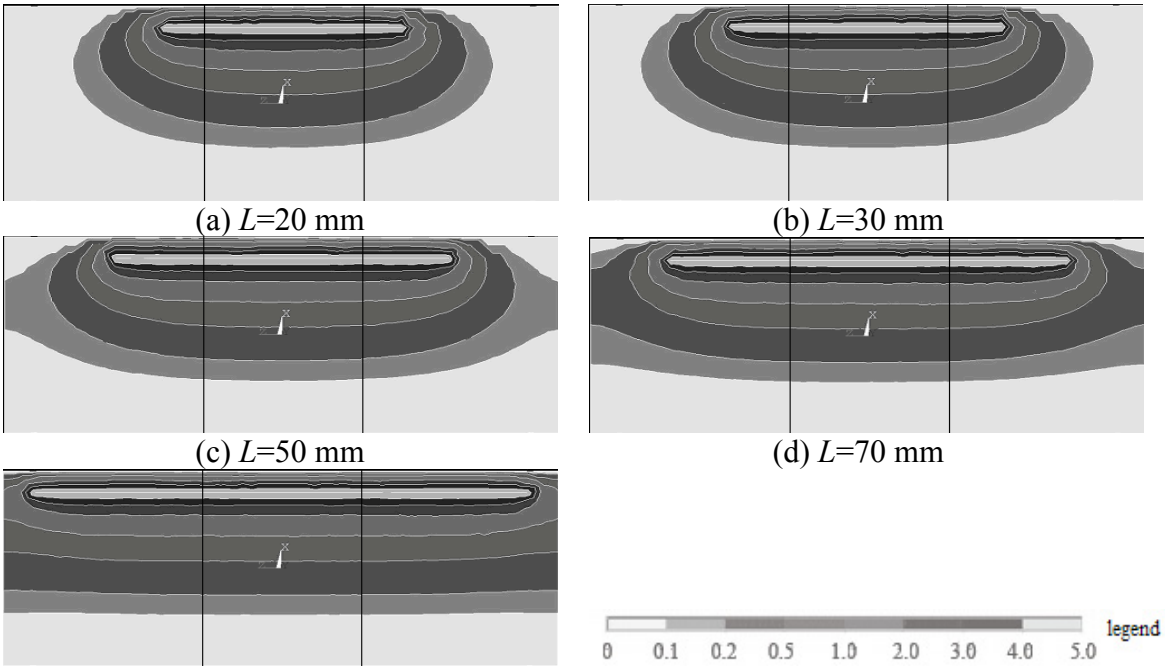

(a) L=20 mm (b) L=30 mm

(c) L=50 mm (d) L=70 mm

(e) L=100 mm

Fig. 5 Potential distribution in the center axial section for five different lengths of guard electrode plate

3.3. Effects of the sensors layout

Potential distribution over cross section with external electrodes system is shown in Fig. 6, with full pipe and empty pipe. The distortion of equipotential contour occurs between the pipe wall and flow medium, and distorted degree varies with different flow medium. This indeterminate potential distribution makes it impossible to evaluate the field sensitivity which is prerequisite to image reconstruction. For internal electrodes system, no distinction has been found between the

potential distribution of full pipe and empty pipe. As the conclusion given by Hussein[3] the pipe wall thickness plays an import role in capacitance sensitivity homogeneity and the consideration about thickness effect is indispensable.

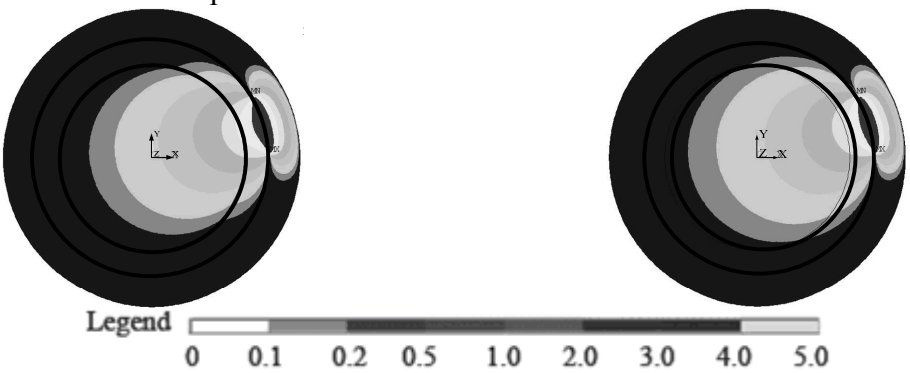

(a) Empty (b) Full

Fig. 6 Potential distribution in the radial section of sensors with external electrode

Comparison of capacitance values of external and internal sensors is listed in Table 1. with some system design parameters below.

pipe wall permittivity $\varepsilon_{pw} = 3.45$ electrode angle: $\theta = 27°$ $L = 100$ mm

$R_1 = 62.5$ mm, $R_2 = 79.5$ mm, $R_3 = 99.5$mm

Table 1 Comparison of capacitance values of internal and external sensors

		C_{1-2}	C_{1-3}	C_{1-4}	C_{1-5}	C_{1-6}	C_{1-7}
Internal	Empty	2.409454	0.090151	0.041005	0.026662	0.021228	0.019751
	Full	3.604968	0.224051	0.102713	0.066788	0.053177	0.049480
	ΔC	1.195514	0.133900	0.061708	0.040126	0.0131949	0.029729
External	Empty	3.555181	0.163814	0.050208	0.029279	0.0225609	0.020838
	Full	3.541350	0.267691	0.111908	0.070372	0.055302	0.051303
	ΔC	**-0.013831**	0.103877	0.061700	0.041093	0.032742	0.030465

Table 1 shows that for a given electrode geometry, the stationary capacitance values for external electrode is larger than those for internal electrode in empty pipe, while in full pipe, the two types of sensors take on almost same capacitance values. As to the capacitance difference between full and empty pipe, a descending tendency is found for internal electrode system. Note that the capacitance variation between an adjoining electrode pair, such as electrode 1 and 2, gives a negative value for external electrode system, this behavior results from so-called soft field effect, in other words, as an ECT system applies an excitation voltage or current，the sensing field is distorted by the target object(s), so that a non-uniform field is induced. The relationship among the capacitance of an electrode pair, C_i, the measured sensitivity distribution function, $S_i(x, y, \varepsilon(x, y))$, and the dielectric distribution in the pipe, $\varepsilon(x, y,)$, is expressed as.

$$C_i = \iint_D \varepsilon(x,y) S_i(x,y,\ \varepsilon(x,y))\ \mathrm{d}x\ \mathrm{d}y \tag{5}$$

where D is the cross section of the pipe. It should be noted that C_i depends on the dielectric distributions in the area where the sensitivity is positive, while negative sensing area corresponding to soft field has to be eliminated during the imageing reconstruction process, this means the number of image data available decreases and the quality of image is dissatisfactory

for predicting final distribution of two components. Therefore internal capacitive sensor system is more suitable for current design than external one.

3.4. Basic Design Scheme

According to above analysis, a capacitance sensor system employed in multiphase flow experimental loop at Daqing oil log detection center has been made. A 1-m-long, 130 mm interior diameter, 14 mm wall thickness acrylic pipe is used as main frame. 12-electrode internal sensors with axial synchro driving guard electrodes (METC) are adopted, which consists of two sets of detecting electrodes. Schematic diagram of basic structure is illustrated in Fig. 7. The 10-cm-long, 3.2-cm-wide, 0.1-mm-thick detecting electrodes fabricated from brass are mounted flush with interior wall with a set of 12 electrodes symmetrically spaced around the circumference of the pipe making up of one imaging level. Two sets, between which one set of 10-mm-long guard electrode is located, are 10 cm apart. The two 5-cm-wide by 10-cm-long guard electrode sets are located flush against the interior wall of the pipe, spaced 5mm left and right to the horizontal edges of two sensing electrode sets. This configuration is to shape and to minimize the interaction by the electrode field linking pairs of detecting electrodes during measurement.

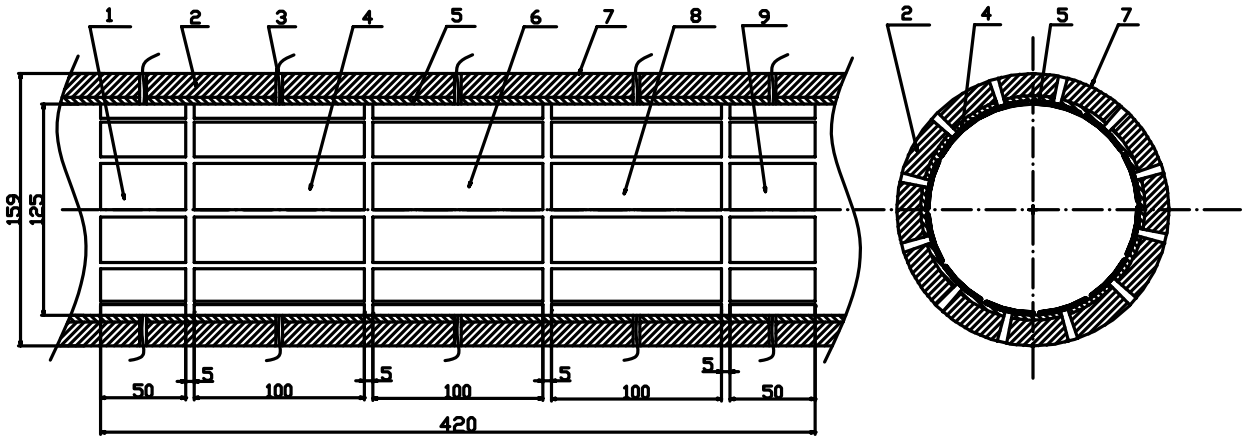

1.6.9. Axial guard electrodes, 2. Acrylic pipe, 3.Lead wire, 4.8.Detecting electrode, 5. Scaleboard, 7. Screen

Fig. 7 Schematic diagram of the capacitance sensor system

3.5. Layout of Electrode Sets

Due to the complexity for the internal capacitance sensors, namely two sets of sensing electrodes and three sets of guard electrodes, totally 60 electrodes are involved in current system, special treatment in layout is required to avoid adverse performance of overall system. All the electrodes are affixed on a polyethylene scaleboard beforehand, and then the scaleboard is rolled up and attached to the interior wall of the pipe.

3.6. Rest of the Design

Since the electrodes are placed inside the pipe, sixty 10-mm-diameter holes were drilled on the acrylic pipe surface, from which wire leads welded to the electrodes came out (Fig. 8). The acrylic pipe was coated with 0.1 mm thick aluminium plate as shield screen to prevent electromagnetic interference from outside, therefore, adequate earthing is necessary.

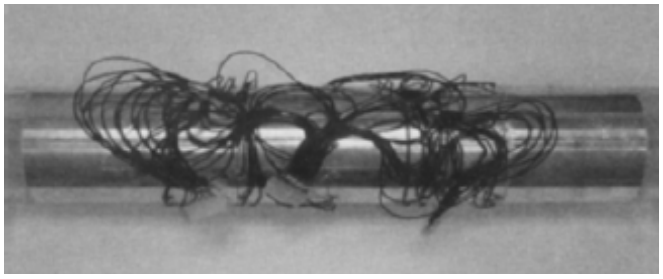

Fig. 8 Picture of capacitance sensor system

4. Conclusion

Three types of capacitance sensors has been simulated and optimized by FE modelling techniques described in this paper. As consequence, a prototype of 12-electrode internal sensors with axial synchro driving guard electrodes (METC) is selected as first part of ECT system used in liquid-gas two-phase flow void fraction measurement. It is demonstrated that performance evaluation and characterization of the capacitance sensor system could be tackled effectively by FE modelling, also simulation results, such as dielectric distribution, might provide prerequisite for successive systems.

References

[1] Hewitt G. F. Handbook of Multiphase system. Hemisphere Publishing, Washington, 1982.
[2] Hewitt G. F. Measurement of two-phase flow parameters. Academic Press, London, 1978.
[3] Hussein E. M. A. and Meneley D. A. Single-exposure neutron tomography of two-phase flow. Int. J. multiphase Flow, 1986, 12:1–34.
[4] Kirouac G. J, Trabold T. A. and Vassallo P. F., Moore W. E., Kumar R. Instrumentation development in two-phase flow. Experimental Thermal and Fluid Science, 1999, 20(2):79–93.
[5] Plaskowski A. B., Beck M. S. and Krawaczynski J. S. Flow imaging for multi-component measurement. Tran. Inst. Meas. Control, 1987, 9:108–112.
[6] Back M. S. PC-Opera User Guide and Reference Manual. Vector Field Limited, Oxford, UK, 1993.
[7] Yang W Q. Modelling of capacitance tomography sensors. IEE Proceedings-Sci. Meas., 1997, 144(5):203–208.
[8] Khan S. H. and Abdullah F. Finite element modelling of multielectrode capacitive systems for flow imaging. IEE Proceedings G, 1993, 140(3):216–222.